

Silicon Cluster Ions: Evidence for a Structural Transition

Martin F. Jarrold and Vladimir A. Constant

AT&T Bell Laboratories, Murray Hill, New Jersey 07974

(Received 26 July 1991)

The mobilities of size-selected silicon cluster ions in helium have been measured using injected-ion drift-tube techniques. The results suggest that a major structural transition occurs for clusters with ~ 27 atoms. Clusters with up to ~ 27 atoms appear to follow a prolate growth sequence, resulting in geometries with an aspect ratio estimated to be ~ 3 . Larger clusters appear to have more spherical shapes. For annealed clusters this structural transition occurs over a narrow size range.

PACS numbers: 61.50.Lt, 36.40.+d

In this Letter we report measurements of the mobilities of silicon cluster ions which suggest that a major structural transition occurs for clusters with around 27 atoms. There is currently intense interest in the physical and chemical properties of semiconductor clusters, particularly silicon clusters [1-9]. Despite the enormous progress that has been made in the last few years, little is known about the structures of silicon clusters containing 10-100 atoms, and the theoretical studies of these clusters are currently the subject of vigorous debate [2-9]. A number of structures have been proposed ranging from a stack of six-membered rings [4,5] to reconstructed fragments of the bulk lattice [7,8]. In many cases the proposed structures have been deduced from chemical-reactivity trends [4-8]. However, it is clear from studies of the reactivity of well-defined surfaces that the relationship between structure, stability, and chemical reactivity does not always follow simple rules [10]. Clearly, a more direct probe of cluster structure is required. Bowers and co-workers [11] have recently shown that it is possible to separate the geometric isomers of carbon cluster ions by their different mobilities. For example, the linear chains, monocyclic rings, and fullerenes can all be separated. The mobility is a measure of how rapidly an ion moves through a buffer gas under the influence of an electric field. For a given cluster size a compact three-dimensional cluster ion will have a larger mobility than a less compact geometry.

The silicon cluster ions for these studies were generated by pulsed laser vaporization of a silicon rod in a continuous flow of helium buffer gas [12]. After exiting the source, the cluster ions were focused into a quadrupole mass spectrometer, where a particular cluster size was selected. The size-selected clusters were then focused into a low-energy ion beam, and injected into a 7.62-cm-long drift tube, containing helium buffer gas at ~ 9 torr. At the end of the drift tube some of the cluster ions exit through a 0.025-cm-diam aperture, and are subsequently mass analyzed by a second quadrupole mass spectrometer. The ions were then detected by an off-axis collision dynode and dual microchannel plates. To measure the drift velocity, an electrostatic shutter is used to allow a 50- μ s pulse of cluster ions to enter the drift tube, and the

arrival time distribution at the detector is recorded with a multichannel analyzer.

Figure 1 shows arrival-time distributions recorded for Si_{22}^+ and Si_{25}^+ . The reduced mobilities K_0 of the cluster ions can be obtained from these results using [13]

$$K_0 = \frac{v_D}{E} \frac{P}{760} \frac{273}{T}, \quad (1)$$

where v_D is the average drift velocity and E is the electric field in the drift tube. All measurements described here were performed in the low-field regime where the drift velocity is directly proportional to the electric field [13]. As can be seen from Fig. 1, a single component is observed in the arrival-time distribution of Si_{22}^+ , indicating that all the Si_{22}^+ clusters have very similar mobilities. For Si_{25}^+ two components are present. Figure 2 shows a plot of the relative mobilities of silicon cluster ions with 10-60 atoms. These relative mobilities were derived by dividing the measured mobility by the hard-sphere mobility, which in turn was obtained from [13]

$$K_{\text{HS}} = \frac{(18\pi)^{1/2}}{16} \left(\frac{1}{m} + \frac{1}{M} \right)^{1/2} \frac{e}{(kT)^{1/2} Q_{\text{HS}}} \frac{1}{N}. \quad (2)$$

In Eq. (2), Q_{HS} is the hard-sphere collision cross section [14], m and M are the masses of the cluster ion and

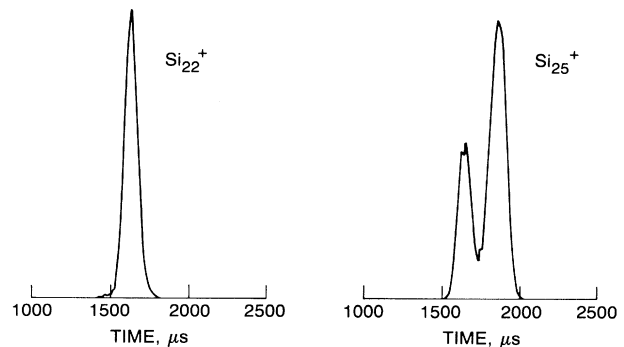


FIG. 1. Arrival-time distributions for Si_{22}^+ and Si_{25}^+ measured at room temperature using a helium buffer gas pressure of 9.8 torr, a drift field of 13.12 V/cm, and an injection energy of 50 eV.

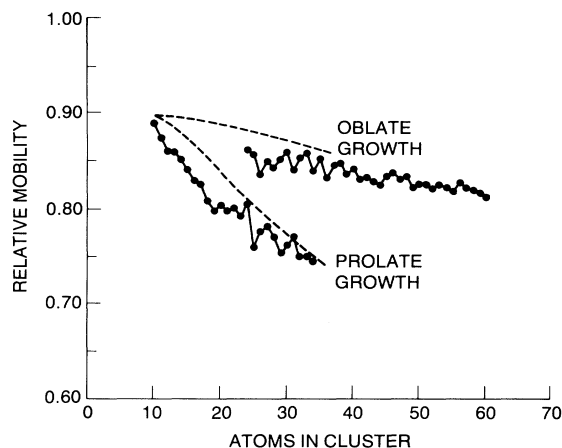


FIG. 2. The relative mobilities (the measured mobility divided by the hard-sphere mobility) against cluster size. These results are an average of two sets of measurements with a typical reproducibility of better than 1%. The dashed lines show the predictions for prolate and oblate growth sequences (see text).

buffer gas, respectively, and N is the buffer gas number density. As can be seen from Fig. 2, the relative mobilities initially decrease with increasing cluster size. Starting at Si_{24}^+ two components are observed in the arrival-time distributions (as shown in Fig. 1 for Si_{25}^+). The second component which appears for $n > 23$ has a larger relative mobility. With increasing cluster size the relative abundance of the component with the smaller relative mobility diminishes and becomes unmeasurable for clusters with $n > 34$.

We have also measured mobilities of some of the silicon cluster ions in neon and argon. With neon the relative mobilities are a few percent smaller than with helium and show the same trends. With argon the relative mobilities are $\sim 30\%$ smaller than with helium. Larger differences between the relative mobilities in helium and argon are generally observed for the smaller clusters. The variations which arise as the buffer gas is changed can be understood in terms of the long-range ion-induced dipole interaction between the silicon cluster ions and the buffer gas. For a point charge the ion-induced dipole interaction is $-ae^2/2R^4$, where a is the polarizability of the neutral species. The polarizabilities of He, Ne, and Ar are 0.205, 0.395, and 1.64 \AA^3 , respectively [15]. Figure 3 shows a plot of the relative mobilities of Si_{25}^+ and Si_{50}^+ in He, Ne, and Ar against the polarizability of the buffer gas. Similar results were obtained for other cluster sizes. With argon, the ion-induced dipole interaction is sufficiently strong that it makes a substantial contribution to the collision cross section, and the measured mobility is significantly smaller than the hard-sphere value. On the other hand, as the polarizability approaches zero the mobility should approach the hard-sphere value. The results shown in Fig. 3 suggest that with helium the polarizability is small enough that the mobilities are within a few

percent of the hard-sphere values.

The most plausible explanation for the variations in the mobilities with cluster size that are apparent in Fig. 2 is that they arise from changes in the shape of the clusters. If a spherical cluster distorts to a prolate top or an oblate top, the relative mobility will decrease because the collision cross section increases. The average collision cross section of a cylinder of length l and diameter $2r$ is

$$Q_{\text{HC}} \approx \frac{1}{2} \pi (r + r_{\text{He}})^2 + \frac{1}{2} \pi (r + r_{\text{He}})(l + r_{\text{He}}). \quad (3)$$

Equation (3) was obtained by averaging over all orientations of the cylinder in space and so we assume that there is no alignment in the drift field. Small alignment effects have been observed [16] with molecular ions but significant alignment is not expected under the low-field conditions employed here. As can be seen from Fig. 2, the mobility of Si_{10}^+ is $\sim 90\%$ of the hard-sphere value suggesting that this cluster is roughly spherical in shape (in agreement with the predictions of molecular-orbital calculations [2]). Starting with the assumption that Si_{10}^+ can be represented by a cylinder with $l = 2r$ [17], we have shown in Fig. 2 the mobilities predicted using the expressions described above, assuming that the clusters grow as prolate tops (constant r) and oblate tops (constant l). Note that the values of l and r have not been optimized to fit the experimental data. Much smaller variations in the mobilities are expected for an oblate growth sequence than for a prolate growth sequence. The experimental results follow the predictions for the prolate growth sequence, suggesting that clusters in this size regime grow as prolate spheroids by addition of atoms preferentially along one of their axes. Using Eq. (3), we estimate from our measurements that this growth sequence results in prolate spheroids with an aspect ratio (defined as $l/2r$) of ~ 3 by Si_{27}^+ . This growth sequence cannot continue indefinitely because of the large surface energy associated with these geometric structures. Eventually the prolate clusters should reconstruct to more spherical shapes to reduce their surface energy. From the results shown in Fig. 2, it appears that this structural transition starts to occur for clusters with 24 atoms, but the prolate ge-

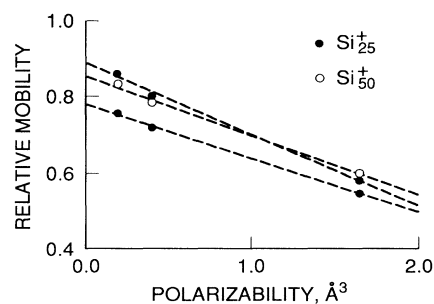


FIG. 3. The relative mobilities of Si_{25}^+ (both components) and Si_{50}^+ measured in He, Ne, and Ar against the polarizability of the buffer gas.

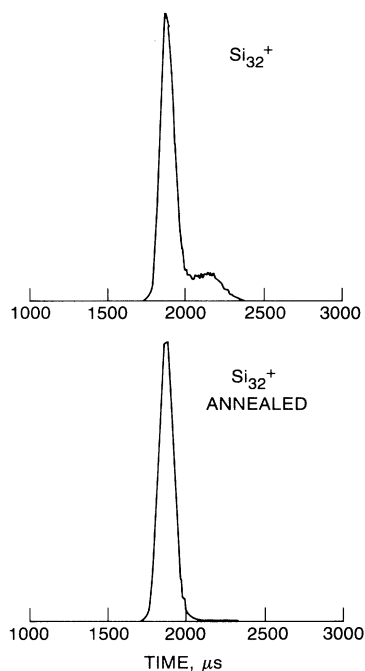


FIG. 4. Arrival-time distributions for Si_{32}^+ . The distributions were recorded with injection energies of 50 eV (upper) and 130 eV (lower).

ometry persists for clusters with as many as 34 atoms.

It may be possible to convert the prolate geometry into the more spherical form by annealing. The clusters can be annealed by injecting them into the drift tube at elevated kinetic energies so that they become excited by collisions with the buffer gas as they enter the drift tube [18]. Figure 4 shows arrival-time distributions recorded for Si_{32}^+ with injection energies of 50 and 130 eV. With the larger injection energy the slower moving component assigned to the prolate geometry has essentially vanished, because it has been annealed into the more spherical form. Clearly, for this cluster the spherical form is considerably more stable than the prolate geometry. Figure 5 shows a plot of the relative abundance of the prolate form as a function of cluster size for both annealed and unannealed clusters. The transition between the two different structural forms occurs over a narrow cluster size range for the annealed clusters. We have previously reported studies of the chemical reactivity of these clusters and showed that isomers, which react with some reagents at different rates, exist for virtually all clusters in the size range examined here [18,19]. In some cases, the structural isomers that can be resolved by their different mobilities can be correlated with isomers observed in our previous chemical-reactivity studies. However, the chemical-reactivity studies indicate isomers are present for many clusters where isomers were not resolved in the arrival-time distributions. Clearly, these isomers must have similar shapes. For many of the larger

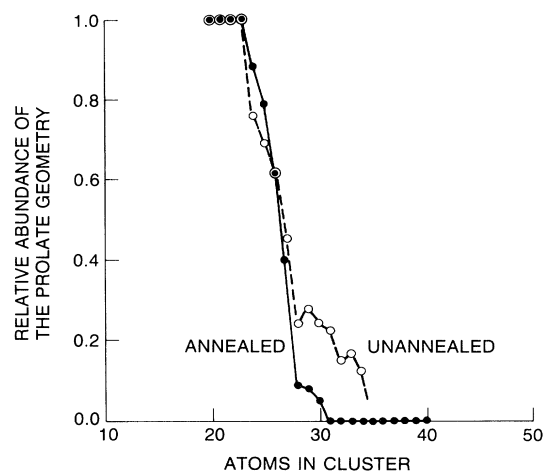


FIG. 5. The relative abundance of the prolate geometry against cluster size for unannealed and annealed clusters.

clusters the arrival-time distributions appear to consist of several unresolved components. For some clusters the arrival-time distributions are clearly asymmetric. Generally, annealing narrows the arrival-time distributions of the larger clusters and the average mobilities increase by a few percent.

There have been many theoretical studies of silicon clusters [2-7]. For clusters with up to 10 atoms probably the most reliable information has come from large-scale molecular-orbital calculations [2]. These clusters have compact, high-coordination number structures that are not fragments of the bulk diamond lattice. The size of the molecular-orbital calculations increases geometrically with cluster size, and for larger clusters less rigorous computational methods must be employed. A wide range of possible structures have been proposed for clusters with 10-100 atoms. The recent work of Chelikowsky, Glassford, and Phillips [20] appears to be qualitatively consistent with our results. These calculations were performed using a classical interatomic force field and simulated annealing methods. According to their calculations, clusters with 20-23 and 25 atoms are prolate spheroids with an aspect ratio of 1.5-2.0 (which is smaller than estimated from our results). Their structures for clusters with 24 and 26-30 atoms are more spherical. The geometries obtained from these calculations are close-packed metalliclike structures. For smaller clusters the molecular-orbital calculations suggest that coordination numbers larger than six are unfavorable [2]. If true, this would provide a strong motivation for adopting a prolate growth sequence because it is possible to avoid overcoordinating any of the atoms in the cluster. We have constructed a number of models of the silicon clusters and found that structures based on a stack of capped trigonal prisms are attractive candidates for the geometries of the prolate clusters with 20-34 atoms. These geometric

structures have approximately the aspect ratio expected from our measurements, the coordination numbers are 3–6, and finally these species can readily lose a Si_{10} unit. Loss of Si_{10} (which is a tetracapped trigonal prism according to the molecular-orbital calculations) is the lowest-energy dissociation pathway for clusters in this size regime [21].

In summary, the mobilities of silicon cluster ions suggest that a major structural transition occurs for clusters with ~ 27 atoms. Clusters with $n > 10$ appear to follow a prolate growth sequence resulting in a geometry with an aspect ratio estimated to be ~ 3 for Si_{27}^+ . Larger clusters appear to have more spherical geometries. The prolate growth sequence may arise as a way to avoid over-coordinating any of the atoms in the cluster. Ultimately, the surface energy of this geometry becomes too large and the clusters reconstruct to a more spherical shape.

We are grateful for helpful discussions with K. Raghavachari, M. L. Mandich, E. C. Honea, and J. E. Bower.

-
- [1] L. Brus, *J. Phys. Chem.* **90**, 2555 (1986); W. L. Brown *et al.*, *Science* **235**, 860 (1987); M. F. Jarrold, *Science* **252**, 1085 (1991).
- [2] K. Raghavachari and C. M. Rohlfing, *J. Chem. Phys.* **89**, 2219 (1989); K. Raghavachari, *Phase Transitions* **24-26**, 61 (1990).
- [3] G. Pacchioni and J. Koutecky, *J. Chem. Phys.* **84**, 3301 (1986); K. Balasubramanian, *Chem. Phys. Lett.* **135**, 283 (1987); C. H. Patterson and R. P. Messmer, *Phys. Rev. B* **42**, 9241 (1990); P. Ballone *et al.*, *Phys. Rev. Lett.* **60**, 271 (1988); R. Biswas and D. R. Hamann, *Phys. Rev. B* **34**, 895 (1986); D. Tomanek and M. Schluter, *Phys. Rev. B* **36**, 1208 (1987); O. F. Sankey *et al.*, *Phys. Rev. B* **41**, 12750 (1990); T. T. Rantala, D. A. Jelski, and T. F. George, *J. Cluster Sci.* **1**, 189 (1990).
- [4] J. C. Phillips, *J. Chem. Phys.* **88**, 2090 (1988).
- [5] D. A. Jelski, Z. C. Wu, and T. F. George, *Chem. Phys. Lett.* **150**, 447 (1988).
- [6] J. R. Chelikowsky and J. C. Phillips, *Phys. Rev. Lett.* **63**, 1653 (1989).
- [7] E. Kaxiras, *Phys. Rev. Lett.* **64**, 551 (1990).
- [8] J. M. Alford, R. T. Laaksonen, and R. E. Smalley, *J. Chem. Phys.* **94**, 2618 (1991).
- [9] W. Andreoni and G. Pastore, *Phys. Rev. B* **41**, 10243 (1990).
- [10] G. A. Somorjai, *Chemistry in Two Dimensions: Surfaces* (Cornell Univ. Press, Ithaca, 1981).
- [11] G. von Helden, M.-T. Hsu, P. R. Kemper, and M. T. Bowers, *J. Chem. Phys.* **95**, 3835 (1991).
- [12] M. F. Jarrold, J. E. Bower, and K. M. Creegan, *J. Chem. Phys.* **90**, 3615 (1989).
- [13] E. W. McDaniel and E. A. Mason, *The Mobility and Diffusion of Ions in Gases* (Wiley, New York, 1973).
- [14] The hard-sphere collision cross sections were derived assuming that the atomic density of the silicon clusters was between that of the diamond form and the β -tin form. The atomic density of the β -tin form is 21% larger than for the diamond form.
- [15] T. M. Miller and B. Bederson, *Adv. Atomic Molec. Phys.* **13**, 1 (1977).
- [16] S. R. Leone, in *Bimolecular Collisions*, edited by M. N. R. Ashford and J. E. Baggott (Royal Society of Chemistry, London, 1989).
- [17] The values of l and r were obtained from the expression $l = 4r_s^3/3r^2$, where r_s is the radius of a sphere of the same volume as the cylinder. r_s is given by $(3nV_a/4\pi)^{1/3}$, where V_a is the atomic volume [14] and n is the number of atoms in the cluster. For Si_{10}^+ these expressions yield a value of $l = 2r = 6.1 \text{ \AA}$.
- [18] M. F. Jarrold and E. C. Honea, *J. Am. Chem. Soc.* (to be published).
- [19] K. M. Creegan and M. F. Jarrold, *J. Am. Chem. Soc.* **112**, 3768 (1990).
- [20] J. R. Chelikowsky, K. M. Glassford, and J. C. Phillips, *Phys. Rev. B* **44**, 1538 (1991).
- [21] Q.-L. Zhang *et al.*, *J. Chem. Phys.* **88**, 1670 (1988); M. F. Jarrold and J. E. Bower, *J. Phys. Chem.* **92**, 5702 (1988); M. F. Jarrold and E. C. Honea, *J. Phys. Chem.* (to be published).